Catal Lett (2012) 142:1128–1133
DOI 10.1007/s10562-012-0863-8

Oxygen Reduction Activity and Methanol Resistance of Ru-based Catalysts Prepared by Solvothermal Reaction

Chuanxiang Zhang · Kazumichi Yanagisawa · Haijun Tao · Aymu Onda · Tatsuo Shou · Sumio Kamiya

Received: 28 February 2012 / Accepted: 11 June 2012 / Published online: 11 July 2012

Abstract Ru-based electrocatalysts were synthesized by the simple one-step solvothermal synthesis method. Catalytic process of oxygen-related species on the surface of the catalysts was investigated by cyclic voltammetry. The oxygen reduction reaction (ORR) activity of Ru–Se/C catalyst, obtained by rotating disk electrode (RDE) technique in O_2-saturated 0.1 M $HClO_4$ solution, was considerably higher than that of Ru–S/C and Ru/C. Moreover, Ru–Se/C exhibited the outstanding methanol-resistant performance in mixed electrolyte of $HClO_4$ and MeOH. The electrochemical result of Ru–Se/C obtained by RDE technique showed the ORR took place by a four-electronic charge transfer process ($n = 4e$).

Keywords Ru-based catalysts · One-step solvothermal synthesis · Oxygen reduction reaction (ORR) · Methanol resistance

C. Zhang
College of Materials Engineering, Nanjing Institute of Technology, Nanjing 211167, China

C. Zhang · K. Yanagisawa (✉) · A. Onda
Research Laboratory of Hydrothermal Chemistry, Faculty of Science, Kochi University, Kochi 780-8520, Japan
e-mail: yanagi@kochi-u.ac.jp

H. Tao
College of Materials Science and Technology, Nanjing University of Aeronautics and Astronautics, Nanjing 210016, China

T. Shou · S. Kamiya
Toyota Motor Corp., Toyota 471-8571, Japan

1 Introduction

It is well known that the direct methanol fuel cell (DMFC) is one of the most promising candidates for a next generation of power sources because of its convenient fuel and portable electronic devices [1]. Two electrodes separated by electrolyte or membrane are most important parts of fuel cell. A fuel is oxidized at the anode, and oxygen reduction reaction (ORR) must take place at the cathode to ensure electroneutrality in the fuel cell. Two different oxygen reduction processes occur at the cathode [2]. The first one is the "direct" four-electron transfer, direct reduction of oxygen to water:

$$O_2 + 4H^+ + 4e \rightarrow 2H_2O, \quad E_0 = 1.23\,V \tag{1}$$

The second one is the "series" mechanism including two-electron transfer as shown by the following equations:

$$O_2 + 2H^+ + 2e \rightarrow H_2O_2, \quad E_0 = 0.68\,V \tag{2}$$

$$H_2O_2 + 2H^+ + 2e \rightarrow 2H_2O, \quad E_0 = 1.77\,V \tag{3}$$

Higher voltage is needed to achieve the effective catalytic reduction of oxygen by the two-electron transfer process, and about 80 % of the overall energy loss in the cell is caused at the cathode because of the complexity of the oxygen reaction process [3]. Platinum, as a catalyst for the cathode of DMFC, gives the efficient direct four-electron transfer pathway but its cost is very high. Therefore, partial or complete replacement of platinum metal attracts much interest to reduce the cost of the products, decrease the market barriers, and enhance the electrocatalytic activity, such as amorphous sulfides catalysts (Ru_xS_y), transition metal chalcogenides with Chevrel phase ($Mo_{6-x}M_xSe_8$), transition metal carbonyl catalysts ($Ru_xS_y(CO)_n$), etc. In 1986, Alonso-Vante

discovered that Ru–chalcogenides could be utilized as an electrocatalyst, and the compound Mo–Ru–Se was prepared by the solid-state reaction method [4]. In 1994, the same group synthesized Ru–chalcogenides by the chemical deposited reaction method with refluxing organic solvents [5], and confirmed that this catalyst exhibited a good performance of resistance to methanol [6, 7]. More importantly, the cost of Ru–chalcogenide catalysts is as low as only 4 % of Pt metal [8].

Here, a simple one-step solvothermal synthesis method was utilized to prepare Ru-based catalysts. It had been proved that the carbon black acted as not only a "supporting substrate", but also "as" a dispersing agent for Ru-based nanoparticles in the one-step solvothermal synthesis method [9]. Catalytic performance of three kinds of catalysts, Ru–Se/C, Ru–S/C and Ru/C, was compared and methanol-resistant performance of ORR process on Ru–Se/C was investigated.

2 Experimental

2.1 Electrocatalyst Preparation

In a typical synthesis process to prepare Ru-based catalysts, 0.25 mmol $Ru_3(CO)_{12}$, carbon black (Ketjenblack EC300J) and 2.25 mmol elemental selenium or sulfur powder were put into a Hastelloy C lined autoclave with inner volume of 20 ml, in which 10 ml i-propanol was filled. After sealed, the autoclave was heated at 150 °C for 10 h and then cooled down to room temperature naturally. $Ru_3(CO)_{12}$ (Ru precursor) should be decomposed at this temperature and then react with selenium or sulfur powder to form Ru–chalcogenides. The precipitate was filtered, washed with acetone, and dried in vacuum. The samples were calcined in a tube furnace (TKS-660, Yamada Denki Co., Japan) at 300 °C for 2 h in a stream of Ar gas. The samples were named as Ru–Se/C or Ru–S/C. Ru/C was prepared with the addition of neither elemental selenium nor sulfur. The carbon content was the same (55 wt%) for the three samples.

2.2 Characterization

A Rigaku Ultima IV X-ray diffractometer with Cu Kα radiation ($\lambda = 1.54056$ Å) was used to obtain X-ray powder diffraction (XRD) data of the samples. The specific surface area was measured by BEL SORP-max ($P/P_0 = 0.1$–0.3 atm). Transmission electron microscopy (TEM) was utilized to observe the morphology and microstructure of the products on Hitachi H-800 instrument working at 200 kV.

The rotating disk electrode (RDE) equipment (HD HOKUTO DENKO) consisted of an automatic polarization system HZ-5000, a dynamic electrode controller HR-300 and a dynamic electrode HR-301. Three-electrode system included a platinum counter electrode, a RHE (HS-250C) reference electrode and a glassy carbon (HR2-D1-GC5) working electrode. Prior to RDE test, the suspension comprised of an electrocatalyst and a small amount of 0.5 wt% Nafion as a binder, was dripped on the surface of the glassy carbon electrode by an injector. The mass density of the target electrocatalyst film cast on the glassy carbon electrode was 10 μg cm^{-2}. Three electrolytes, 0.1 M $HClO_4$, a mixed electrolyte of 0.1 M $HClO_4$ + 1.0 M MeOH and 1.0 M $HClO_4$, were used in this study.

3 Results and Discussion

3.1 Physical Properties

The as-prepared samples obtained by solvothermal reactions before the calcination had no definite X-ray diffraction peaks except the broad diffraction of the carbon at about $2\theta = 25°$ [10]. Figure 1a showed the XRD patterns of the three catalysts after the calcination at 300 °C. The broad peaks marked with asterisks in the samples Ru–Se/C, Ru–S/C and Ru/C were formed by the calcination and might correspond to Ru_xSe_y, Ru_xS_y and Ru_x, respectively, according to the decarboxylation reaction as shown in the following equations [11]:

$$Ru_3(CO)_{12} + ySe \rightarrow Ru_xSe_y + zCO \quad (4)$$

$$Ru_3(CO)_{12} + yS \rightarrow Ru_xS_y + zCO \quad (5)$$

$$Ru_3(CO)_{12} \rightarrow Ru_x + zCO \quad (6)$$

When the samples were calcined at higher temperatures such as 450 °C (Fig. 1b), $RuSe_2$ (JCPDS Card No. 03-1198), RuS_2 (JCPDS Card No. 19-1107) and high crystalline Ru metal (JCPDS Card No. 06-0663) were formed in Ru–Se/C, Ru–S/C and Ru/C catalysts, respectively.

Figure 2 showed the morphology of C, Ru/C, Ru–S/C and Ru–Se/C observed by TEM. The TEM images of Ru/C, Ru–S/C and Ru–Se/C directly showed that the deep black colored slipcover were observed on the carbon support. They must correspond to Ru, Ru_xS_y, and Ru_xSe_y, respectively. Agglomeration of Ru metal with low crystallinity easily led to uneven dispersion on carbon surface, which was shown by red circles in the TEM image (Fig. 2b). In Ru–S/C, the carbon particles seem to be enlinked with each other by the deposition of Ru_xS_y. The dispersive uniformity of Ru_xSe_y was considerably higher

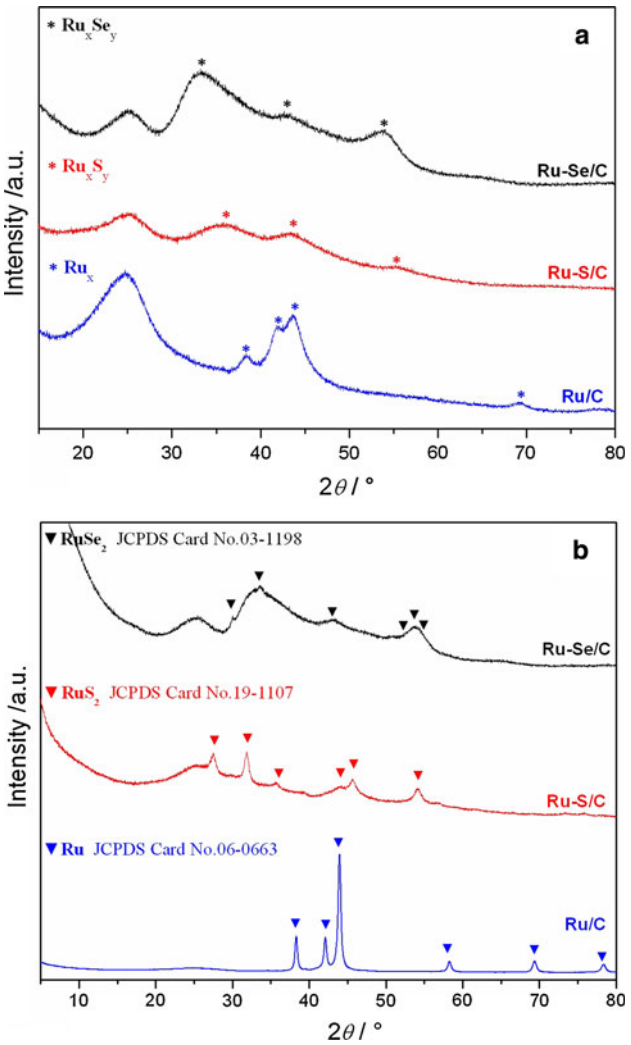

Fig. 1 XRD patterns of Ru–Se/C, Ru–S/C and Ru/C calcined at **a** 300 °C and **b** 450 °C

than Ru_xS_y catalyst. The specific surface areas of Ru/C (221.0 $m^2\ g^{-1}$), Ru–S/C (298.2 $m^2\ g^{-1}$) and Ru–Se/C (416.4 $m^2\ g^{-1}$) may support this observation.

Ru–Se/C was observed by high-resolution transmission electron microscope (HRTEM) to verify the dispersion and particle size of the catalyst supporting on the carbon. Figure 3 presented HRTEM image of Ru–Se/C catalyst. The uniform dispersion of Ru_xSe_y catalyst supporting on carbon surface could be observed. The dark parts in the carbon fringe must be Ru_xSe_y particles, though they were not very clearly distinguished probably resulting from low crystallinity. However, their particle size could be estimated to be less than 5 nm. These results indicated that the addition of selenium was effective in preventing the particle aggregation, and the one-step solvothermal synthesis method provided the carbon supported catalyst with small ruthenium-based selenide particles.

3.2 Cyclic Voltammetry

Cyclic voltammetry curve reflected the adsorption, desorption and reduction of O_2 on the surface of the electrodes as shown in Fig. 4. Catalytic process of oxygen-related species could be shown in Scheme 1 according to Yeager [2], where "M" represented the catalyst. Thus, the small and broad anodic current peak, which began at ~0.40 V (vs. RHE) and was amplified at 0.70 V (vs. RHE), was caused by adsorption of oxygen-related species such as hydroxyl species, to form surface oxides on Ru–Se/C catalyst. The cathodic peak at 0.50 V (vs. RHE) was attributed to reduction of surface oxides. Comparing with Ru–S/C and Ru/C, larger current in a small range of voltage drop reflected more rapid kinetic catalytic process of oxygen-related species for Ru–Se/C catalyst.

3.3 Oxygen Reduction Reaction Activity

The results of ORR measurements for Ru–Se/C, Ru–S/C, Ru/C and Pt/C catalysts in O_2-saturated 0.1 M $HClO_4$ solution by the RDE technique are shown in Fig. 5. For the Ru/C and Ru–S/C catalysts (blue triangles and red circles in Fig. 5, respectively), the increase in cathodic disk current density resulted from the reduction of O_2 commenced at almost the same potential, ~0.55 V (vs. RHE). However, the disk current density of Ru–S/C was larger than that of Ru/C, which might be explained by its higher specific surface area (298.2 $m^2\ g^{-1}$) comparing with that of Ru/C (221.0 $m^2\ g^{-1}$). For Ru–Se/C catalyst (black squares), the reduction of O_2 commenced at much more positive potential, 0.80 V (vs. RHE), which could be attributed to metallic Se bonding with Ru [12]. The disk current density for Ru–Se/C catalyst was obviously increased. Larger disk current density of Ru–Se/C might be caused by uniform dispersion of Ru–Se particles and a large increase of the specific surface area to 416.4 $m^2\ g^{-1}$. The other reason for the obvious ORR difference between Ru–S/C and Ru–Se/C might be given by the difference of the crystallinity of the samples. The XRD patterns of the samples (Fig. 1) show clearly that Ru–Se/C consists of low crystalline $RuSe_2$ but Ru–S/C is amorphous. Thus Ru–Se/C showed a better performance in catalytic property compared with the other two catalysts.

The onset potential for the Pt/C catalyst was about 0.87 V vs. RHE in 0.1 M $HClO_4$, slightly higher than that of our sample Ru–Se/C. However, our catalyst may have a potential value because the cost for Pt is much higher than that of our catalyst. Recently a three-component RuFeSe chalcogenide catalyst with electrocatalytical activity comparable to that of Pt was prepared [13], which suggests that the property of our catalyst might be improved by further

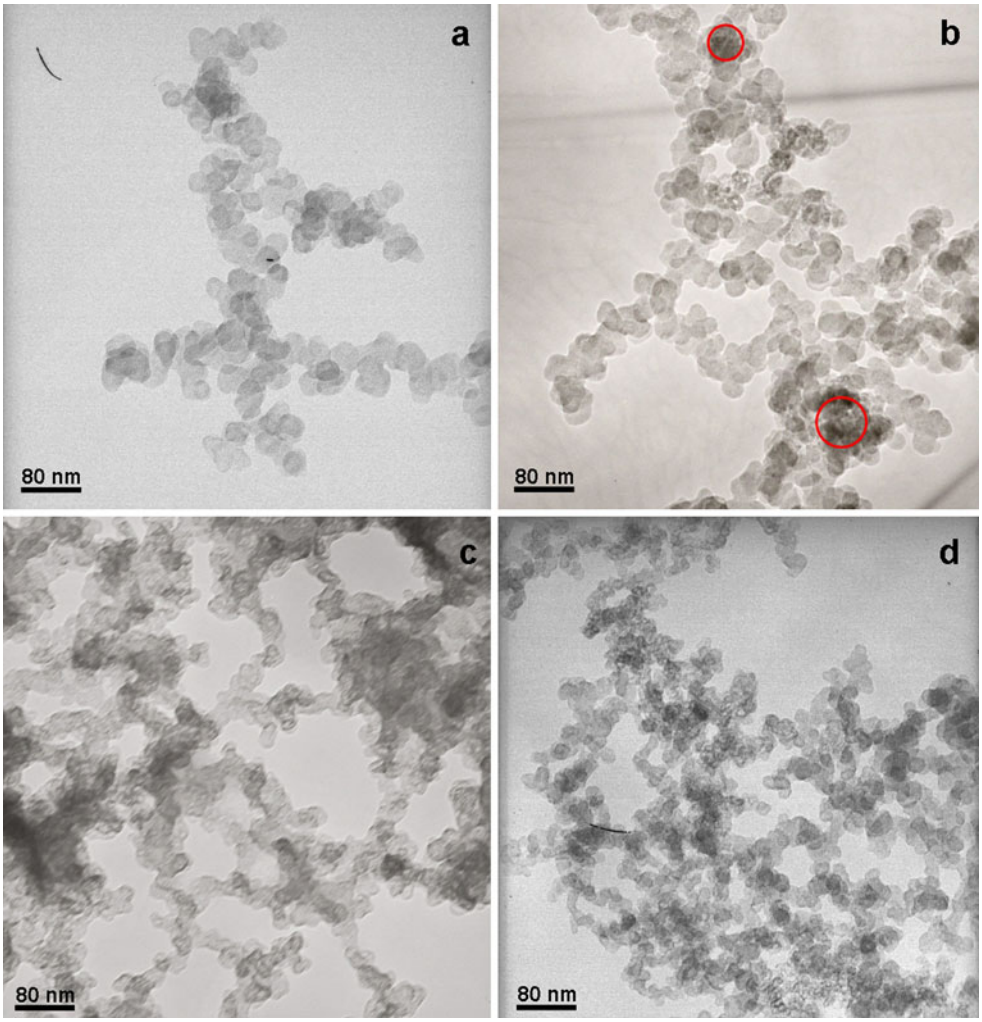

Fig. 2 TEM images of **a** C, **b** Ru/C, **c** Ru–S/C and **d** Ru–Se/C

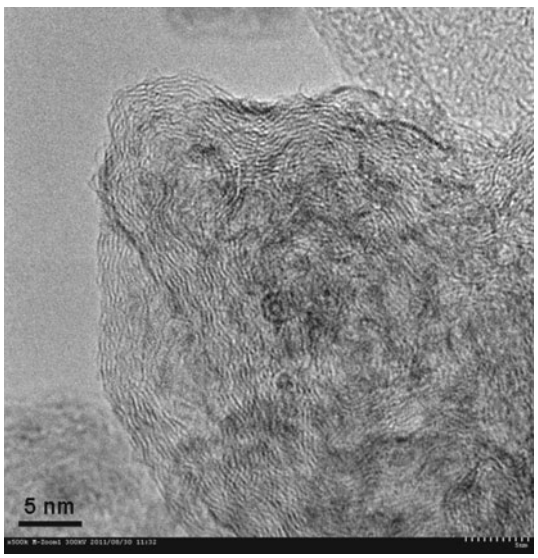

Fig. 3 HRTEM image of Ru–Se/C catalyst

controlling the preparation conditions including the addition of additives.

3.4 Methanol Resistance of Ru–Se/C Catalyst

To observe the methanol-resistant performance of Ru–Se/C, a current–potential curve of Ru–Se/C was obtained in a mixture of 0.1 M $HClO_4$ and 1.0 M CH_3OH, and was compared with that in 0.1 M $HClO_4$ (Fig. 6). The ORR activity in the mixed electrolyte was almost same to that measured in $HClO_4$, which suggested that Ru–Se/C catalyst obviously exhibited outstanding methanol-resistant performance. The excellent methanol tolerant capability may expand the feasibility of application of Ru–Se/C catalyst to DMFC.

3.5 Electron Transfer in ORR

Figure 7 shows typical current–potential curves for the Ru–Se/C catalyst at five different rotation rates by scanning the

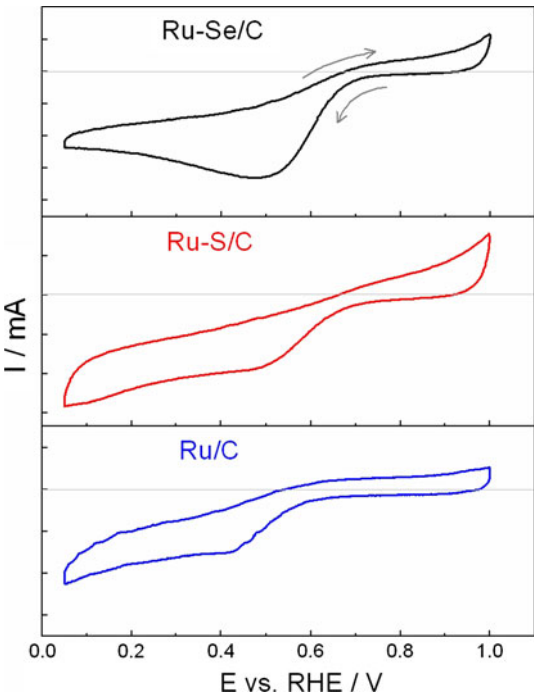

Fig. 4 Cyclic voltammetry curves of Ru–Se/C, Ru–S/C and Ru/C in O_2-saturated 0.1 M $HClO_4$. Scanning rate: 15 mV s^{-1}

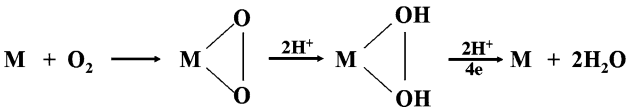

Scheme. 1 Schematic diagram of catalytic process of oxygen-related species on the surface of electrode [2]

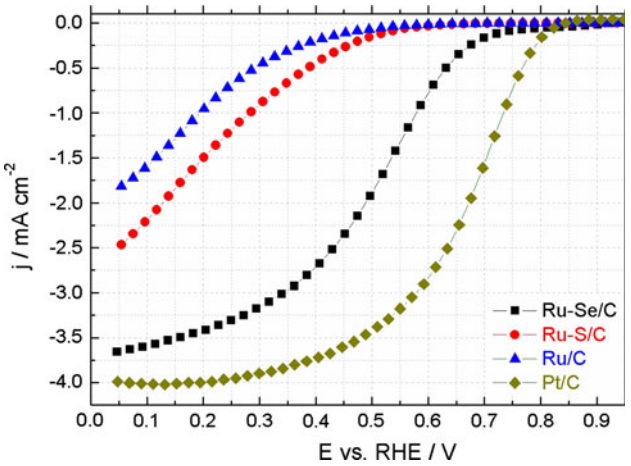

Fig. 5 Typical current–potential curves of Ru–Se/C, Ru–S/C, Ru/C and Pt/C in O_2-saturated 0.1 M $HClO_4$. Scanning rate: 15 mV s^{-1}, rotation rate: 1,600 rpm

potential from the open circuit potential at a scanning rate of 15 mV s^{-1} in 1.0 M $HClO_4$. Characteristic charge-transfer kinetics control results in no significant variation

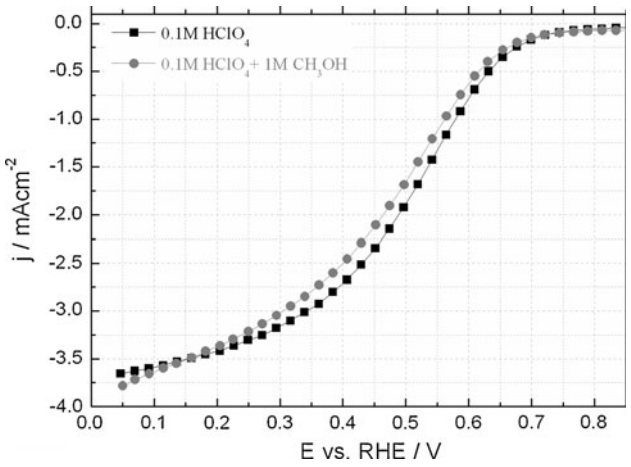

Fig. 6 Typical current–potential curves of Ru–Se/C in O_2-saturated 0.1 M $HClO_4$ and 0.1 M $HClO_4$ + 1 M CH_3OH electrolyte. Scanning rate: 15 mV s^{-1}, rotation rate: 1,600 rpm

of the currents with the different rotation rates in the region between 0.70 and 0.85 V (vs. RHE). At more cathodic potentials, a mixed control in the range 0.70–0.45 V (vs. RHE) is observed, in which a well-defined limiting current depends on rotation rate of the electrode. With increasing rotating speed, the limiting currents are increased owing to the increase of oxygen diffusion through the electrode surface [14].

The disk current density, j, of the oxygen reduction can be related to the kinetic current density, j_k, and the diffusion-limited current density, j_d [15] by

$$\frac{1}{j} = \frac{1}{j_k} + \frac{1}{j_d} \tag{7}$$

The diffusion-limited current density can be expressed as

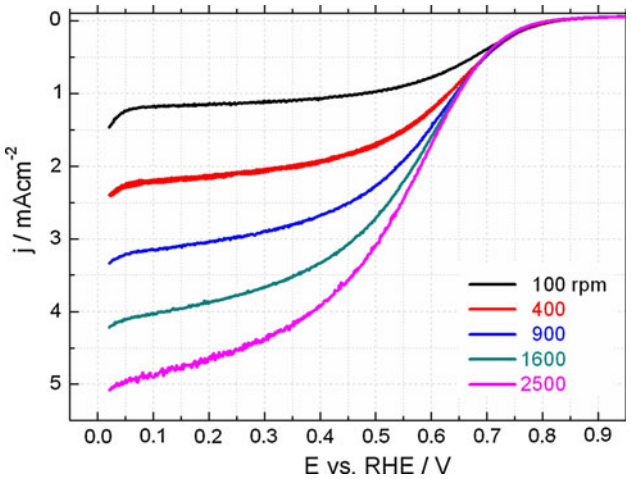

Fig. 7 Typical current–potential curves for Ru–Se/C in O_2-saturated 1.0 M $HClO_4$ at different rotation rates. Scanning rate: 15 mV s^{-1}

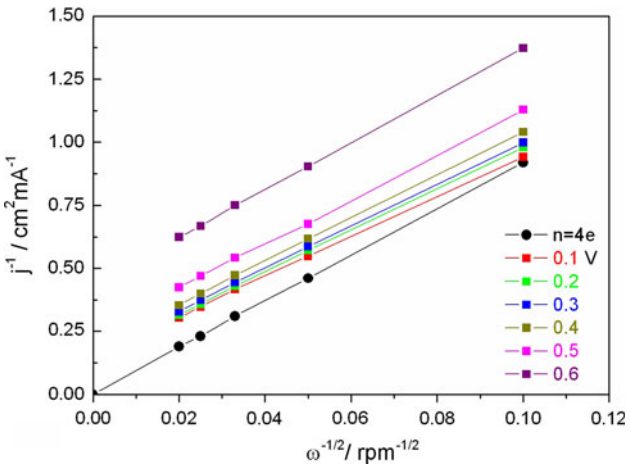

Fig. 8 Koutecky-Levitch plots for Ru–Se/C catalyst at different electrode potentials obtained from Fig. 7

$$j_d = 0.2\, n_e F\, Co\, Do^{2/3}\, v^{-1/6}\, \omega^{1/2} = B\, \omega^{1/2} \tag{8}$$

where 0.2 is a constant used when ω is expressed in rotations per minute (rpm), n_e the number of electrons transferred per molecule of O_2 in the overall reaction, F the Faraday constant (96,485 C mol^{-1}), Co the concentration of dissolved oxygen (1.6×10^{-6} mol cm^{-3}), Do the diffusion coefficient of oxygen in the solution (1.1×10^{-5} cm^2 s^{-1}), v the kinematic viscosity of perchloric acid (1.0×10^{-2} cm^{-2} s^{-1}) and B the Levich constant [16]. Therefore, the current for oxygen reduction can be written as

$$\frac{1}{j} = \frac{1}{j_k} + \frac{1}{B}\omega^{-1/2} \tag{9}$$

Koutecky-Levitch plots (j^{-1} versus $\omega^{-1/2}$) for Ru–Se/C catalyst at different electrode potentials are shown in Fig. 8 from the data in Fig. 7. At all the rotation speeds, parallelism of the straight lines in Fig. 7 indicated that the number of electron transferred per O_2 molecule and active surface area for the reaction did not change significantly within the potential range studied in this work [17]. The theoretical average value of the Levich slope, B, was calculated to be 1.12×10^{-3} mA cm^{-2} $rpm^{-1/2}$ when $n_e = 4$. The experimental value of B from the average slopes of Fig. 8 was found to be 1.06×10^{-3} mA cm^{-2} $rpm^{-1/2}$ and was quite close to the theoretical value. From these results, it could be concluded that the O_2 reduction of Ru–Se/C catalyst proceeds via the overall four-electron transfer reaction to water formation according to equation (1), as had been reported on the basis of the same logical relationship [18].

4 Conclusions

In conclusion, the electrocatalysts, Ru–Se/C, Ru–S/C and Ru/C, were prepared by the simple and efficient one-step solvothermal synthesis method, and it was found that Ru–Se/C catalyst exhibited faster reaction kinetics and higher catalytic performance compared with the other two catalysts. The enhancement of the electrochemical property of Ru–Se/C catalyst might be explained by good dispersion of catalyst particles on carbon, larger specific surface area and metallic bonding of Se with Ru. There was a great potential for Ru–Se/C catalyst to apply on DMFC due to its outstanding methanol resistance even in electrolytes including high concentrations of methanol. It was confirmed that the O_2 reduction of Ru–Se/C catalyst proceeded via the desired "direct" four-electron transfer reaction to water.

Acknowledgments This work was supported by Japan Society for the Promotion of Science, Grant-in-Aid for Scientific Research (B) 21350116.

References

1. Kim S, Cho MH, Lee JR, Park SJ (2006) J Power Sources 159:46
2. Yeager E (1984) Electrochim Acta 29:1527
3. Toda T, Igarashi H, Uchida H, Watanabe M (1999) J Electrochem Soc 146:3750
4. Alonso-Vante N, Tributsch H (1986) Nature 323:431
5. Solorza-Feria O, Ellmer K, Giersig M, Alonso-Vante N (1994) Electrochim Acta 39:1647
6. Alono-Vante N, Tributsch H, Solorza-Feria O (1995) Electrochim Acta 4:567
7. Fischer C, Alonso-Vante N, Fiechter S, Tributsch H (1004) J Appl Electrochem 1995:24
8. Feng Y (2008) Phys Status Solidi 9:1792
9. Zhang C, Yanagisawa K, Tao H, Onda A, Shou T, Kamiya S (2011) Catal Lett 141:1311
10. Gullá AF, Gancs L, Allen RJ, Mukerjee S (2007) Appl Catal A Gen 326:227
11. Alonso-Vante N (2006) Fuel Cells 6:182
12. Babu PK, Lewera A, Chung JH, Hunger R, Jaegermann W, Alonso-Vante N, Wieckowski A, Oldfield E (2007) J Am Chem Soc 129:15140
13. Delacôte C, Lewer A, Pisarek M, Kulesza PJ, Zelenay P, Alonso-Vante N (2010) Electrochim Acta 55:7575
14. Suárez-Alcántara K, Solorza-Feria O (2008) Electrochim Acta 53:4981
15. Nekooi P, Amini MK (2010) Electrochim Acta 32:86
16. Hsueh KL, Gonzalez ER, Srinivasan S (1983) J Electroanal Chem 153:79
17. Suárez-Alcántara K, Rodríguez-Castellanos A, Dante R, Solorza-Feria O (2006) J Power Sources 157:114
18. González-Cruz R, Solorza-Feria O (2003) J Solid State Electrochem 7:289